Temperature dependence of betavoltaic cell performance of diamond *pn* junction diode

Takehiro Shimaoka, Hitoshi Umezawa, Gwenole Jacopin, Satoshi Koizumi, Takeshi Fujiwara, Julien Pernot

***Abstract*— Temperature dependence of the energy conversion efficiency of diamond *pn* junction betavoltaic cells was evaluated. We fabricated pseudo vertical diamond *pn* junction diode and characterized its energy conversion efficiency under electron beam irradiation from 5-300 K. The diamond *pn* junction diode exhibits energy conversion efficiencies of 18-24% at 150-300 K, which is more than twice as high as those of silicon PiN diode. On the other hand, below 100 K, the energy conversion efficiency of the diode significantly drops due to the increase of series resistance of diamond. Above 150K, the diamond *pn* junction diode presents smaller temperature dependency on energy conversion efficiency than that of silicon diode, which would make diamond *pn* junction betavoltaic cells, a promising device for energy harvesting in remote sensing devices over a wide temperature range except in the cryogenic region.**

***Index Terms*—ultrawide bandgap, energy conversion, nuclear battery, betavoltaic cell, remote sensing**

I. Introduction

Betavoltaic cells convert beta-particles emitted from radioactive isotopes into energy. They work by a principle similar to that of solar cells. Its advantage is longevity. The lifetime of the battery depends on the half-life of the beta emitting isotopes. Therefore, they can operate for several decades to more than one hundred years[1], [2]. The disadvantage of the betavoltaic cells is low power output density compared to that of solar cells, ranging from a few to several hundred nW/cm^2. Therefore, they can be used where sunlight does not reach and battery replacement becomes a major cost, for example, outer planets, the deep sea, and implantable devices.

One of the most important performance indicators of betavoltaic cells is the energy conversion efficiency. From a Shockley-Queisser (SQ) model for betavoltaics, it has been predicted that the conversion efficiency increases with increasing band gap[2], [3]. From this perspective, wide bandgap materials are promising for betavoltaic batteries, and the development of nuclear batteries (betavoltaics, alphavoltaics, X-ray and Gammavoltaics) using SiC, GaN, and InGaP *pn* diodes, and diamond Schottky barrier diodes have been reported[4]–[10]. We have previously demonstrated extremely high energy conversion efficiencies for diamond *pn* diode at room temperature under electron-beam irradiation[11]. In this study, we investigated the temperature dependence on betavoltaic performance of diamond *pn* junction diode from room temperature to cryogenic temperatures.

II. Experimental

A. Sample preparation

We fabricated a pseudo vertical diamond *pn* junction diode. Figure 1 shows the schematic of the diode. We used HPHT Ib (111) single-crystal diamond as the substrate. The p^+, p, n^-, and n^+ layers were epitaxially grown on the substrate by microwave plasma CVD. The thickness, and impurity concentration of each layer was evaluated by secondary ion mass spectrometry (SIMS). The thickness of the p^+, p, n^-, and n^+ layer was >1.5μm, 0.1μm, 3.5μm, and 0.1μm, respectively. Impurity concentration of each layer was [B]:2×10^{19} atoms/cm^3, [B]:1×10^{17} atoms/cm^3, [P]: 5×10^{16} atoms/cm^3, and. [P]:1×10^{20} atoms/cm^3. Subsequently, a mesa structure with a diameter of Ø240μm was formed by induction coupling plasma etching. After forming the mesa structure, Ti/Mo/Au ohmic electrodes were formed on the n^+ and p^+ layers by EB deposition.

B. Characterizations

Current-voltage (*I-V*) characteristics of the pseudo-vertical diamond *pn* diode under electron irradiation were evaluated using a Source Measure Unit (Keithley2611). For electron-beam irradiation, a scanning electron microscopy (SEM, FEI Inspect F50) system was used. The voltage range was set from -2 V to +6 V and the voltage step was 10 mV. The above measurements were repeated between 300 K and 5 K. For comparison, similar measurements were performed with a Si-PiN diode (S3590-09, Hamamatsu photonics K.K.). Active area

This paragraph of the first footnote will contain the date on which you submitted your paper for review. This work was supported by JSPS KAKENHI grant number JP21K18000

T. Shimaoka, H. Umezawa, are with the National Institute of Advanced Industrial Science and Technology (AIST), Midorigaoka, Ikeda,Osaka Japan (e-mail:shimaoka.takehiro@aist.go.jp, hitoshi.umezawa@aist.go.jp).

T. Fujiwara is with the National Institute of Advanced Industrial Science and Technology (AIST), Tsukuba, Ibaraki Japan (e-mail: fujiwara-t@aist.go.jp).

G. Jacopin, and J. Pernot, are with Univ. Grenoble Alpes, CNRS, Institut Néel, 38000 Grenoble, France(e-mail: gwenole.jacopin@neel.cnrs.fr, julien.pernot@neel.cnrs.fr).

S. Koizumi is with the National Institute for Materials Science (NIMS), Ibaraki 305-0044, Japan (e-mail: koizumi.satoshi@nims.go.jp).

of the Si-PiN diode is 10×10mm^2.

Figure 2 shows the depth profiles of the electron beam energy deposit estimated using the Monte Carlo simulation software CASINO[12]. Here, we set an electron beam acceleration voltage $V_{acc.}$ = 17.4 kV, assuming a Ni-63 electron source (average electron energy of 17.4 keV). The penetration depth of the electron beam is 2 μm for diamond, and 3 μm for silicon. In diamond pseudo vertical structure, most of the energy is deposited in the n^--layer. The electron beam reflectance r was 3% for diamond and 14% for silicon. The irradiation dose of the electron beam was adjusted to match the short-circuit current density expected when Ni-63 beta source was used[3], [13]. The average electron flux in the diode and the deposited energy were estimated from Faraday cup current (I_{sc}) and acceleration voltage($V_{acc.}$). The value was set to 1.1×10^{11} electrons/cm^{-2}s^{-1} for diamond diode and 6.9×10^{9} electrons/cm^{-2}s^{-1} for silicon PiN diode. Note that, the irradiated electron flux of the diamond diode was an order of magnitude higher than that of silicon PiN diode, even with the smallest beam aperture of the SEM due to the small diameter of diamond *pn* junction diode.

From the obtained *P-V* and *I-V* curves, the short-circuit current (I_{sc}), open-circuit voltage (V_{oc}), and maximum output power (P_{mp}) were obtained. Then fill factor (FF), charge collection efficiency (Q) and energy conversion efficiency (η) were calculated using the following equations.

$$FF = \frac{P_{mp}}{V_{oc} I_{sc}} \cdots (1)$$

$$Q = I_{sc} / I_{EHP} \cdots (2)$$

$$I_{EHP} = (1-r)\frac{V_{acc.} I_{FC}}{\varepsilon} \cdots (3)$$

$$\eta = (1-r)Q\frac{V_{oc} FF}{\varepsilon} \ldots (4)$$

,where ϵ is the electron–hole pair creation energy. We substituted 13 eV for diamond and 3.6 eV for silicon[14], [15]. I_{EHP} is the current in the diode induced by electron beam irradiation.

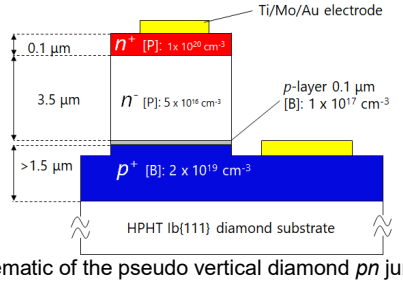

Fig. 1. Schematic of the pseudo vertical diamond *pn* junction diode

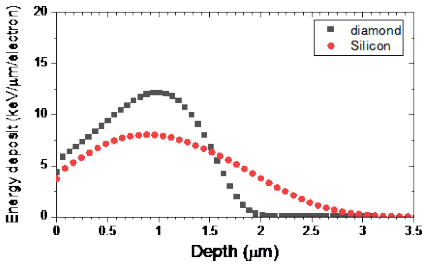

Fig. 2. Depth profile of the electron beam energy deposit

III. Results and Discussions

Figure 3(a) and (b) show the *P-V* and *I-V* characteristics of diamond *pn* junction diodes at room temperature to 5 K. The V_{oc} and P_{mp} increased when temperature decreased. At 150 K, the output power was 1.4 times greater than that at 300 K. Below 100 K, the I_{sc} started to decrease, and at 5 K it was less than one-tenth of that at room temperature. Figure 4(a) and (b) shows the *I-V* and *P-V* characteristics of silicon PiN diodes. Data points at 200 K and 5 K were missing due to poor contact of the probe. The maximum output power also increased as the temperature decreased and it became by a factor of 8 from room temperature to 50 K.

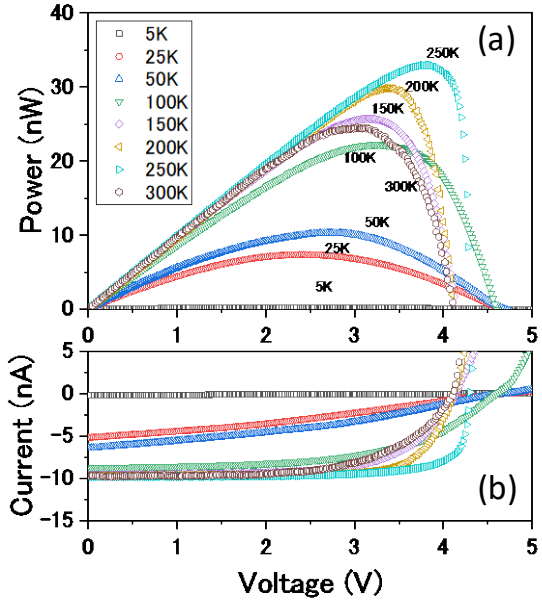

Fig. 3. (a) *P-V* and (b) *I-V* characteristics of diamond *pn* junction diodes at 5 K to 300 K.

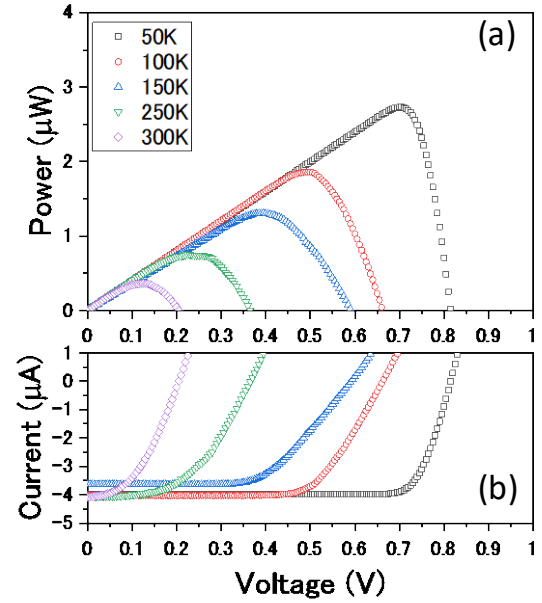

Fig. 4. (a) *P-V* and (b) *I-V* characteristics of Si-PiN diode from 50 K to 300 K.

Figure 5 (a)-(e) shows the temperature dependencies of η, Q, FF, V_{op}, and series resistance R_s of diamond and Si-PiN diodes. For Si-PiN diode, η, FF, and V_{oc} were monotonically increased with decreasing sample temperature. For diamond, η reached a

maximum at 250 K and decreased at the lower temperatures. This may be due to the reduction in forward leakage current caused by the lowering of the barrier height of *pn* junction due to epitaxial defects, and the improvement in *FF*. Between 150-300 K, the change of *FF* strongly contributes to the trend of η. Since diamond has >4V of large V_{oc}, the contribution of the *FF* improvement due to the increase in V_{oc} caused by the decrease of sample temperature was comparatively small compared to silicon. Although the CCE remained at zero bias voltage, the gradient near the open circuit voltage of *I-V* curve decreased, which degraded the *FF*. This could be due to a decrease in minority carrier diffusion length of diamond with decreasing temperature. Below 100K, a significant decrease in CCE was observed, and it was nearly zero at 5K. The series resistance of the diode calculated from the gradient of the forward characteristics exceeded 10MΩ, which may be limiting the current. Although a decrease in CCE due to exciton formation has been reported at cryogenic temperatures, the electric field formed at the *pn* junction is >10 kV/cm, which is sufficient to dissociate a portion of excitons[16]. Thus, exciton formation cannot describe drastically CCE drops below 50K. By reducing the series resistance of the diode fabricating a vertical structure, optimizing doping concentration for resistivity and minority carrier diffusion length, it may be possible to mitigate the decrease in energy conversion efficiency even at cryogenic temperatures.

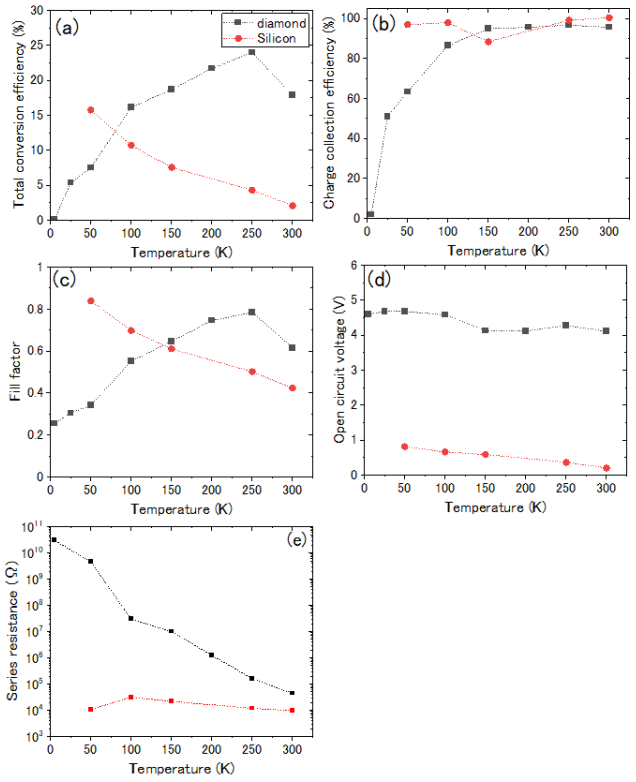

Fig. 5. Betavoltaic parameters of diamond *pn* and Si-PiN diodes with various temperature. (a)Total conversion efficiency(η), (b)Charge collection efficiency(Q), (c)*Fill factor(FF), (d)open circuit voltage(V_{oc}),* and (e) series resistance(R_s).

Comparing the temperature dependence of η between diamond and silicon, from 300-150 K, the η of the diamond *pn* diode changed by a factor of 1.4. If the leakage component of the diode is suppressed, the variation can be even smaller. In silicon PiN diode, there was a change by a factor of 3.6. Below 100 K, the difference in energy conversion efficiency between diamond and silicon became smaller. Since the temperature dependence of diamond is small, betavoltaic cells using ultrawide bandgap materials are expected to maintain high energy conversion efficiency over a wide temperature range, especially in the high temperature region. In addition to the above features, in environments where irradiation damage to semiconductors from high-energy gamma-rays, neutrons, and heavy charged particles is a problem, there is a possibility that power generation can continue for a longer period using diamond devices, which have higher radiation tolerance compared to silicon devices[17].

In this study, we have focused on characterization on energy conversion efficiency of the diamond *pn* diode, however, the power output is proportional to the active area and volume of the device for practical use. In diamond diodes, as the device size increases, leakage current of the diodes tend to increase due to defects caused by epitaxial growth, substrates, and other device processing.[9], [18] We will progress the classification of device killer defects and the demonstration of large-area diamond *pn* junction diodes as the future work.

IV. Conclusion

We evaluated the temperature dependence of the betavoltaic performance of the diamond *pn* diode. From 150 K to 300 K, diamond exhibits more than twice of high energy conversion efficiency than that of silicon. Below 100 K, the energy conversion efficiency decreased drastically due to the drops in short circuit current. Above 150 K, diamond presents lower temperature dependence of energy conversion efficiency (1.4 times) than that of silicon (3.6 times). Diamond *pn* junction diode is promising as a power conversion device with high energy conversion efficiency.

Acknowledgment

The authors would like to thank Dr. Fabrice Donatini of Institut Néel for the setup of SEM and EBIC measurement systems.

References

[1] L. C. Olsen, P. Cabauy, and B. J. Elkind, “Betavoltaic power sources,” *Phys. Today*, vol. 65, no. 12, pp. 35–38, Dec. 2012, doi: 10.1063/PT.3.1820.

[2] L. C. Olsen, “N94-11407 REVIEW OF BETAVOLTAIC ENERGY CONVERSION.”

[3] S. I. Maximenko, J. E. Moore, C. A. Affouda, and P. P. Jenkins, “Optimal Semiconductors for 3H and 63Ni Betavoltaics,” *Sci. Rep.*, vol. 9, no. 1, p. 10892, Jul. 2019, doi: 10.1038/s41598-019-47371-6.

[4] C. Thomas, S. Portnoff, and M. G. Spencer, “High efficiency 4H-SiC betavoltaic power sources using tritium radioisotopes,” *Appl. Phys. Lett.*, vol. 108, no. 1, p. 013505, Jan. 2016, doi: 10.1063/1.4939203.

[5] C. Honsberg, W. A. Doolittle, M. Allen, and C. Wang, “GaN betavoltaic energy converters,” *Conf. Rec. IEEE Photovolt. Spec. Conf.*, pp. 102–105, 2005, doi: 10.1109/pvsc.2005.1488079.

[6] C. D. Cress, B. J. Landi, R. P. Raffaelle, and D. M. Wilt, "InGaP alpha voltaic batteries: Synthesis, modeling, and radiation tolerance," *J. Appl. Phys.*, vol. 100, no. 11, 2006, doi: 10.1063/1.2390623.

[7] S. Butera, M. D. C. Whitaker, A. B. Krysa, and A. M. Barnett, "Temperature effects on an InGaP (GaInP) 55Fe X-ray photovoltaic cell," *Sci. Rep.*, vol. 7, no. 1, pp. 1–8, Dec. 2017, doi: 10.1038/s41598-017-05181-8.

[8] C. Delfaure, M. Pomorski, J. de Sanoit, P. Bergonzo, and S. Saada, "Single crystal CVD diamond membranes for betavoltaic cells," *Appl. Phys. Lett.*, vol. 108, no. 25, p. 252105, Jun. 2016, doi: 10.1063/1.4954013.

[9] V. Bormashov *et al.*, "Development of nuclear microbattery prototype based on Schottky barrier diamond diodes," *Phys. status solidi*, vol. 212, no. 11, pp. 2539–2547, Nov. 2015, doi: 10.1002/pssa.201532214.

[10] G. R. Mackenzie *et al.*, "A diamond gammavoltaic cell utilizing surface conductivity and its response to different photon interaction mechanisms," *Mater. Today Energy*, vol. 21, p. 100688, 2021, doi: 10.1016/j.mtener.2021.100688.

[11] T. Shimaoka, H. Umezawa, K. Ichikawa, J. Pernot, and S. Koizumi, "Ultrahigh conversion efficiency of betavoltaic cell using diamond pn junction," *Appl. Phys. Lett.*, vol. 117, no. 10, 2020, doi: 10.1063/5.0020135.

[12] D. Drouin, A. R. Couture, D. Joly, X. Tastet, V. Aimez, and R. Gauvin, "CASINO V2.42 - A fast and easy-to-use modeling tool for scanning electron microscopy and microanalysis users," *Scanning*, vol. 29, no. 3, pp. 92–101, 2007, doi: 10.1002/sca.20000.

[13] R. Zheng *et al.*, "Understanding efficiency improvements of betavoltaic batteries based on 4H-SiC, GaN, and diamond," *Appl. Phys. Lett.*, vol. 121, no. 10, 2022, doi: 10.1063/5.0102995.

[14] F. Nava, C. Canali, C. Jacoboni, L. Reggiani, and S. F. Kozlov, "Electron effective masses and lattice scattering in natural diamond," *Solid State Commun.*, vol. 33, no. 4, pp. 475–477, 1980, doi: 10.1016/0038-1098(80)90447-0.

[15] T. Shimaoka *et al.*, "Fano factor evaluation of diamond detectors for alpha particles," *Phys. Status Solidi Appl. Mater. Sci.*, vol. 213, no. 10, pp. 2629–2633, 2016, doi: 10.1002/pssa.201600195.

[16] D. Cosic, G. Provatas, M. Jakšić, and D. Begušić, "Charge collection efficiency of scCVD diamond detectors at low temperatures," *Diam. Relat. Mater.*, vol. 127, no. June, 2022, doi: 10.1016/j.diamond.2022.109184.

[17] B. Liu *et al.*, "Alpha-voltaic battery on diamond Schottky barrier diode," *Diam. Relat. Mater.*, vol. 87, no. February, pp. 35–42, 2018, doi: 10.1016/j.diamond.2018.05.008.

[18] H. Umezawa, Y. Mokuno, H. Yamada, A. Chayahara, and S. Shikata, "Characterization of Schottky barrier diodes on a 0.5-inch single-crystalline CVD diamond wafer," *Diam. Relat. Mater.*, vol. 19, no. 2–3, pp. 208–212, Feb. 2010, doi: 10.1016/j.diamond.2009.11.001.